Kochi Chapter

Indian Geotechnical Conference
IGC 2022
15th – 17th December, 2022, Kochi

Deformation Mode of Geocell-Soil Composite Structure

Kuldeep T. Sankhat[1][0000-0001-9149-0321], Jitesh T. Chavda[2][0000-0003-0396-5759], Ashish Juneja[3][0000-0001-6544-0857]

[1] Undergraduate Student, Department of Civil Engineering, Sardar Vallabhbhai National Institute of Technology Surat, Surat 395007
[2] Assistant Professor, Department of Civil Engineering, Sardar Vallabhbhai National Institute of Technology Surat, Surat 395007
[3] Professor, Department of Civil Engineering, Indian Institute of Technology Bombay, Mumbai 400 076

Abstract. This paper discusses to develop a three dimensional (3D) numerical model which can effectively simulate the behavior of geocell reinforced soils using a commercial finite element program. In the usual instance, numerical modelling of geocell is difficult due to their curved geometry and complex material surfaces. It is therefore not surprising that much of the previous studies on geocell have eluded this approach and have otherwise used an equivalent composite method. It treats the geocell-soil composites as a new soil layer with improved strength and stiffness properties. Unfortunately, despite its simplicity, this method can often be incorrect as it does not properly account for the state of insitu stress in the soils. Plane stress conditions are also violated especially when the geocell are placed close to the ground surface. Likewise, the shape of the geocells also affect the working of geocell. In the present study, the reinforced soil layer considers the interaction between the geocell and its nodes at connections. Geocell are modelled using poly-curves available in the software. Three types of simulations are then made, they are: reinforced soil with geocell and unreinforced soil, rectangular geocell with curvilinear geocell, and geocell with different axial stiffness. It was seen that the secant modulus of the reinforced soils increases with the increase in the curvature of the geocell. And as the axial stiffness of the geocell material increases, the secant modulus of the reinforced soil also improves.

Keywords: Geocell reinforced soil, soil anisotropy, numerical modelling.

1 Introduction

1.1 Introduction to Geocell

From a very long time, humans are using reinforcement (bamboo or reed) to make clay wall surface, to make a road over soft soil, etc. However, Vidal's (1969) pioneering work has led to a significant rise in interest in this topic. The basic characteristics of reinforced earth and Engineers are drawn to it because of its general economy and ease of manufacture, as well as its simplicity. Earlier, the concept of reinforcing the earth

was particularly associated with metallic reinforcements. Planar reinforcement in metallic strips and meshes has been extensively used to improve foundations, roads, and wall construction for the last four decades worldwide.

The following stage in this field employs geocell to create 3D confinement to the soil. The geocell foundation mattress is made up of interlocking cells reinforced with polymer geogrid that efficiently retain and constrain the soil. It intercepts possible failure planes and forces them deeper into the foundation soil, hence enhancing bearing capacity. The United States Army Corps of Engineers was the first to use and patent geocell in the early 1980s. The technology was first applied to constructing roadways across soft soils for military purposes. Geocell is now utilized for foundation stabilization and erosion control on slopes and channels and retaining wall construction.

1.2 Introduction to Reinforced Soil

Geosynthetic sheets or strips of galvanized steel are used to systematically reinforce the soil in the field of civil engineering. It is primarily because such reinforced soil has many novel properties that make it ideal for constructing geotechnical structures. The reinforcement is simple to handle, store, and install. The locally available soil can be used to fill the geocell and to compact the soil system using modern compaction equipment's.

Based on how the geosynthetics reinforcement absorbs soil stresses and the types of stresses it absorbs, the load-carrying mechanism of geocell can be broadly understood with the help of following mechanisms (Shukla, 2002, 2004 and Shukla and Yin, 2006):

1. A geosynthetics layer reduces shear load, or outward horizontal stresses, that are transferred from the top of the fill or covering soil to the base of the foundation soil and this mechanism is known as the shear stress reduction effect. This effect results in a general-shear failure as opposed to a local-shear failure, increasing the foundation soil's ability to support more weight. The geosynthetics can enhance the system performance with little to no rutting thanks to the shear contact mechanism. At modest deformations, the geosynthetics layer's main advantage is a change in failure mode brought on by low shear stress.
2. A layer of geocell redistribute the surface load that is coming on it as geocell constrain the granular fill which result in the reduction of normal stress acting on the foundation. This effect is known as the slab effect (confinement effect).
3. As the edges of geocell are anchored and once geocell is deformed, geocell will impart vertical resistance to the overlying soil and this mechanism is known as the membrane effect.
4. Interlocking of the soil through the aperture openings of the geocell wall is one of the major benefits of geocell. Due to less surface area and higher aperture size, interlocking mechanism generally dominant compared to friction, but exception occur when the size of soil particles is small in which interlocking effect is negligible.

1.3 Material Used for Geocell

HDPE (High-density polyethylene) and Neoloy, a novel polymeric alloy (NPA) is the two materials generally used as a material for geocell. HDPE-based geocell exhibit high creep and low elastic modulus (stiffness) over time, especially when subjected to high dynamic loads.

Around 15 years ago, global collaborative research between the commercial sector and academics triggered an increase in basic research on geocell. These investigations resulted in a better understanding of the reinforcement methods and performance characteristics required for heavy load pavement applications which show that geocell must have high elastic modulus and creep resistance so that it could maintain the shape of the cell which in turn maintain confinement under dynamic stresses. The second result was the development of Neoloy, a novel polymeric alloy (NPA) for geocell, to meet these engineering requirements of geocell. That is NPA has high elastic stiffness, minimal permanent deformation, and high tensile strength. The third outcome was a better understanding of how Neoloy-based geocell perform in pavement applications.

2 Numerical Modelling

PLAXIS 3D is a three-dimensional finite element analysis application that analyses the deformation and stability of various geotechnical situations. Soil models can be created in two modes: soil mode and structure mode. The staged construction mode simulates construction and excavation processes by allowing to activate and deactivate soil volumes and structural elements, apply loads, consider the water table, and other features. The PLAXIS output, among other things, allow to determine the deflections, stresses, and safety factor of the geotechnical problem.

The model generated in soil and structures mode is converted into tetrahedron components, including nodes, and mesh generation is accomplished based on the nodes in PLAXIS programming. Analysis can be known at any time because of the production of the nodes; the entire model is built up of triangular components and nodes, whereas in finite-difference programs, the basic element is a square or rectangle, which implies that the nodes at the ends cannot be formed exactly.

Table 1: Properties of soil used in the analysis

Parameter	Soil
Material Model	Mohr-Coulomb
Drainage type	Drained
Unit weight above phreatic level(kN/m^3)	17
Unit weight below phreatic level(kN/m^3)	18
Youngs modulus (kN/m^2)	1×10^4
Poisson's ratio	0.3
Cohesion (kN/m^2)	10
Friction Angle(degree)	30
Dilatancy Angle(degree)	0
K_0 determination	Automatic
Lateral earth pressure coefficient	0.5

The properties of soil used in the study is provided in Table 1. The foundation plate of size 1m x 1m is provided to represent the concrete foundation of M25 grade having a Young's modulus of 25 x 10^6 kPa. The geocell with different values of axial stiffness (400, 800, 1200, 1600, 2000) kN/m are used, and then the FE simulations are run.

In PLAXIS 3D, the *Fine mesh* option is used for the *Element Distribution* to generate the mesh. The mesh is locally refined at the area where the load is applied with the coarseness factor of 0.32. The remaining boundary is refined with a Coarseness Factor of 0.8. The schematic representation of position of geocell, boundary dimensions, application of the load is shown in Figure 1. The study output is observed at nine nodes as shown in figure. They are: (0,0,0), (-0.5,0,0), (0.5,0,0), (0,0, -0.2), (-0.5,0, -0.2), (0.5,0, -0.2), (0,0, -0.35), (-0.5,0, -0.35), (0.5,0, -0.35).

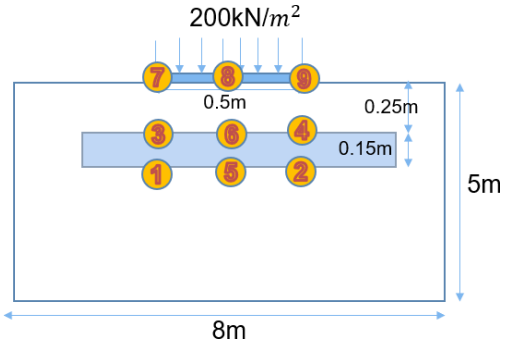

Figure 1: Nodes position in the model

3 Results and Discussion

3.1 Interpretation of the Result

In the study, the results are presented in the form of a stress-strain curve. The stiffness of the soil is strengthened if the increase in the secant modulus of the stress-strain curve is observed. The stress-strain curve is plotted corresponding to the specific node. The Curves with the same color represent that both are calculated at the same node, provided one of the curves with a dash line, and the other with a solid line.

3.2 Case 1: Soil Reinforced with Geocell and Unreinforced Soil

The image of the rectangular geocell which is used in the study is shown in **Figure 2**. Whereas, the complete 3D model depicting the geocell reinforced soil is shown in **Figure 3**. The comparison between unreinforced soil and reinforced soil with rectangular geocell is obtained for the case under consideration. On the foundation plate, a load of 200 kN/m^2 is applied.

The stress strain behavior of the unreinforced and reinforced soil with rectangular geocell is provided in Figure 4. Dash line represent unreinforced soil and solid line represents geocell reinforced soil. Curve having similar color represent same node. Out of nine nodes, for this case, for ease of understanding, only two nodes are taken for

clear representation. It can be seen that the secant modulus of reinforced soil at each node (2 nodes in this case (-0.5,0, -0.2), (-0.5,0, -0.35)) is higher than unreinforced soil. Thus, it can be inferred here that with the addition of geocell, the stiffness of the ground is improved.

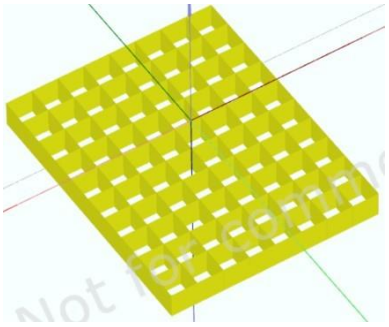

Figure 2: Rectangular geocell

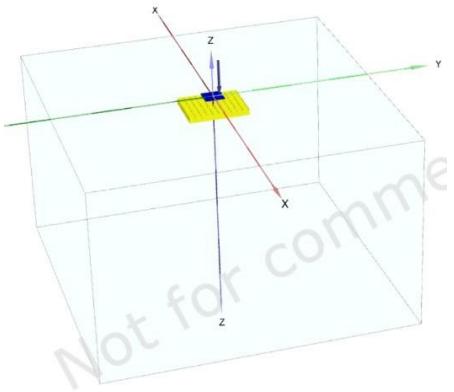

Figure 3: Rectangular geocell reinforced model

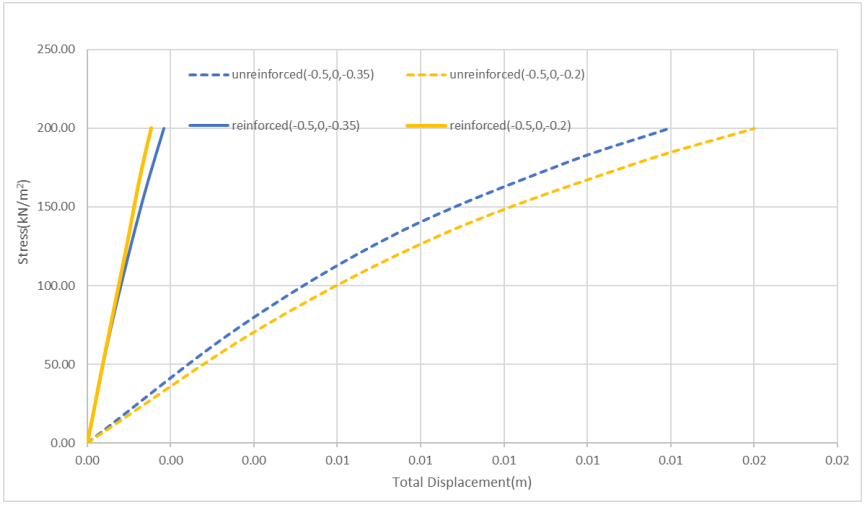

Figure 4: Stress-strain behaviour of unreinforced and reinforced rectangular geocell (Case 1)

3.3 Case 2: Comparison between rectangular and curvilinear geocell

An attempt is made to create the shape of the geocell as close as the shape of real-life honeycomb geocell. **Figure 5** shows the shape of the geocell used in this model, for this case 2. **Figure 6** shows the complete 3D model of the curvilinear geocell reinforced soil. In case 2, the comparison between rectangular and curvilinear geocell is made. Soil is reinforced with curvilinear geocell and on reinforced soil, the

foundation plate is assigned with the load of 200kN/m^2. For this case also, two nodes are considered to plot the graph (see Figure 7). As per Figure 7, the secant modulus of the curvilinear geocell is higher than the rectangular geocell, which implies that the curvilinear geocell are able to provide better stiffness to soil compared to the rectangular geocell.

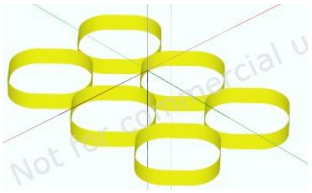

Figure 5: Curvilinear geocell

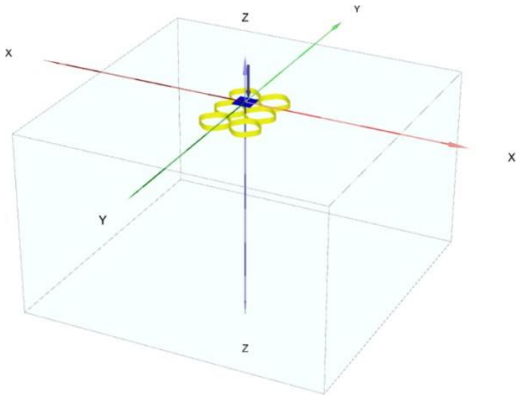

Figure 6: Curvilinear geocell reinforced soil

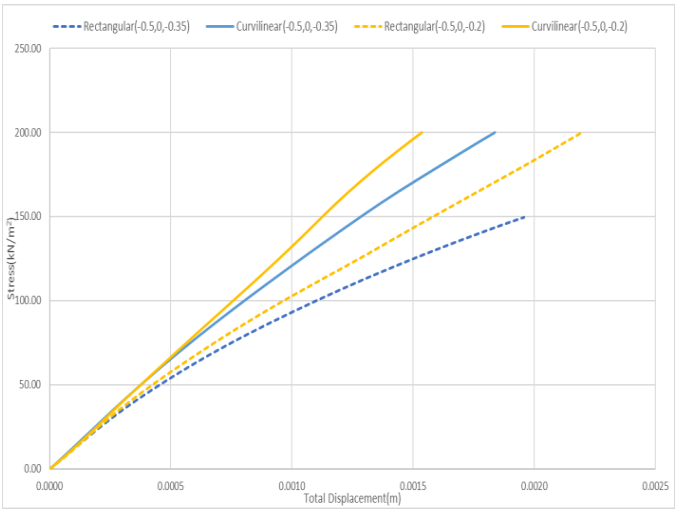

Figure 7: Stress-strain behaviour of reinforced rectangular and curvilinear geocell (Case 2)

3.4 Case 3: Comparison of Geocell with different Axial Stiffness

Case 3.4.1: Axial Stiffness 400 and 800 kN/m

In this case, the curvilinear geocell with an axial stiffness of 400 kN/m is compared with that of the geocell with the axial stiffness of 800 kN/m. In **Figure 8**, a comparison of the stress-strain curve is shown for reinforced soil with curvilinear geocell material with an axial stiffness of 400 kN/m and 800 kN/m.

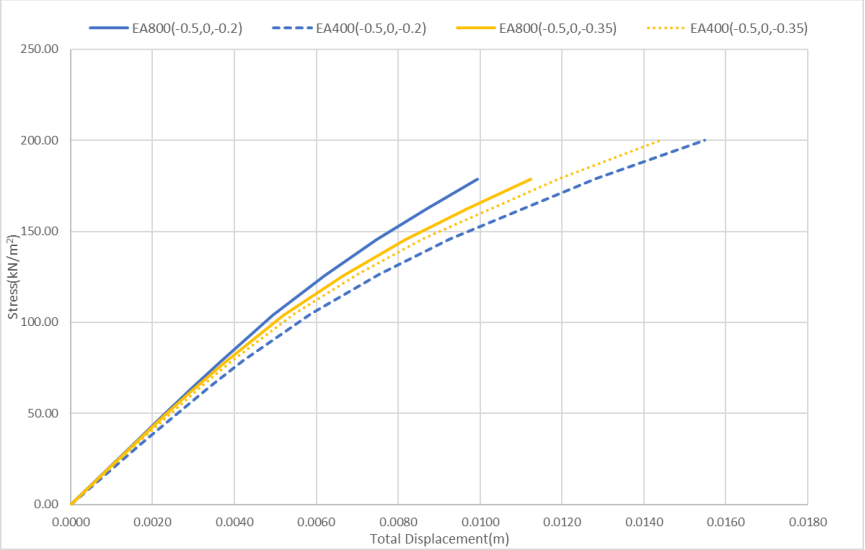

Figure 8: Stress-strain behaviour of reinforced curvilinear geocell with an axial stiffness of 400 and 800 kN/m at (-0.5,0, -0.2) and (-0.5,0, -0.35)

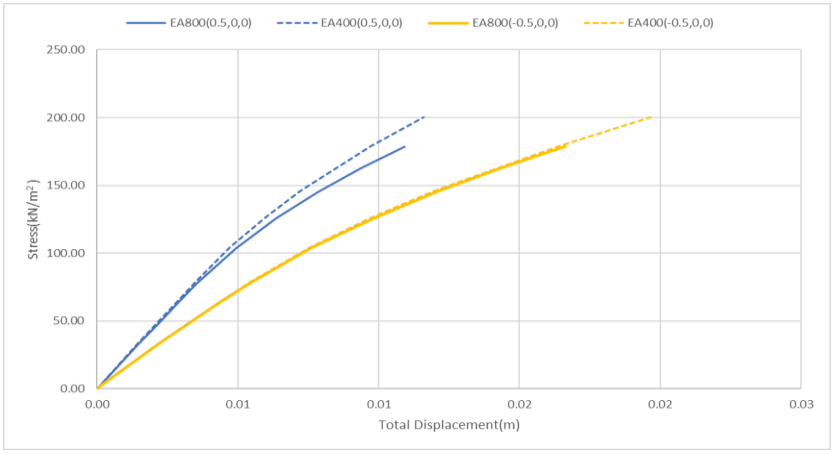

Figure 9: Stress-strain behaviour of reinforced curvilinear geocell with an axial stiffness of 400 and 800 kN/m at (0.5,0,0) and (-0.5,0,0)

In **Figure 8** and **Figure 9**, dash line represents reinforced soil with geocell having an axial stiffness of 400 kN/m, while solid line represents reinforced soil with geocell having axial stiffness equal to 800 kN/m. The stress-strain plot for **Figure 8** is corresponding to nodes (-0.5,0, -0.2) and (-0.5,0, -0.35) and for Figure 9 is corresponding to nodes (0.5,0,0) and (-0.5,0,0). It is observed that there is a significant improvement in the secant modulus of geocell with EA 800 compared to that of EA 400 on some nodes (i.e., at the two nodes given in **Figure 8**); however, there are some nodes where the difference is not significant and also where EA 400 is better than EA800. In **Figure 9**, two exceptions are listed, which states that the geocell with EA 400 is better than the geocell with EA 800. Out of nine nodes, three exceptions are found ((0.5,0,0), (-0.5,0,0) and (0,0,-0.2)) (EA 400 > EA 800), three nodes ((-0.5,0,-0.2), (-0.5,0,-0.35) and (0.5,0,-0.2)) are found at which the improvement is significant, and at rest three, there is very little improvement which is still, however, not significant ((0.5,0,-0.35), (0,0,0) and (0,0,-0.35)).

Case 3.4.2: Axial Stiffness 400 and 1200 kN/m

In this case, the geocell with an axial stiffness of 400 kN/m is compared with that of the geocell with an axial stiffness of 1200 kN/m. From **Figure 10**, it can be seen that the secant modulus on the usage of EA 1200 is higher than that of the reinforced soil in which geocell with the axial stiffness of 400 kN/m is used.

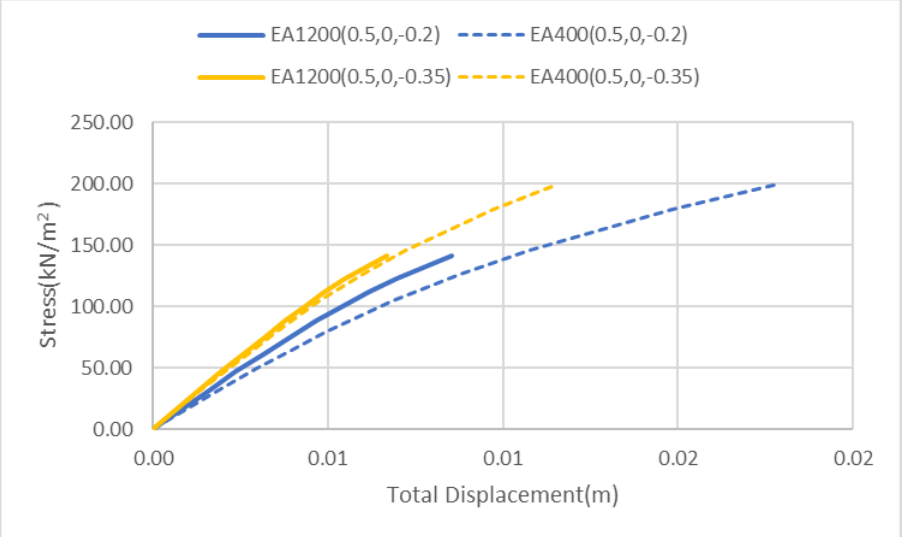

Figure 10: Stress-strain behaviour of reinforced curvilinear geocell with an axial stiffness of 400 and 1200 kN/m at (0.5,0, -0.2) and (0.5,0, -0.35)

Apart from three points where there is a significant improvement in secant modulus, there is one node ((-0.5,0, -0.2)) where reinforced soil with EA 400 geocell's secant modulus is higher than that of the reinforced soil with secant modulus is 1200 kN/m (**Figure 11**). Apart from this single node (**Figure 11**), all other eight nodes have higher

secant modulus, out of which two nodes ((0.5,0, -0.2) and (0.5,0, -0.35)) have significant improvement while the rest of the six nodes has not mush significant or little improvement.

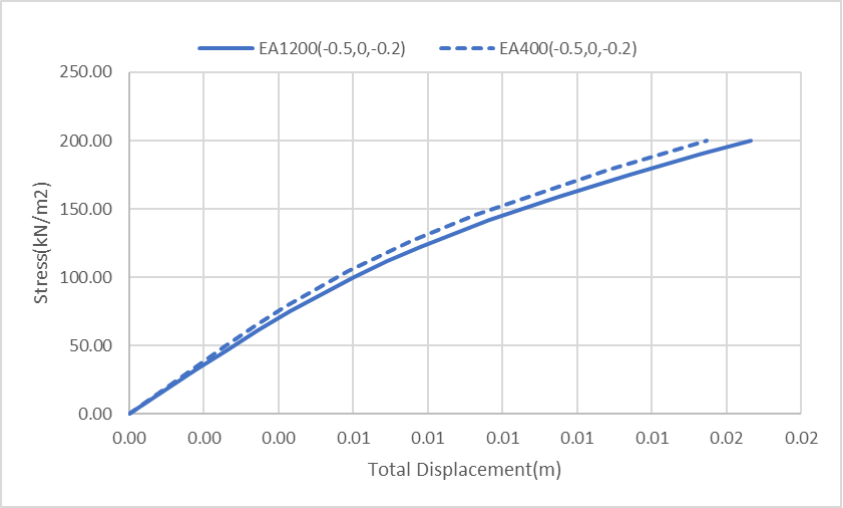

Figure 11: Stress-strain behaviour of reinforced curvilinear geocell with an axial stiffness of 400 and 1200 kN/m at (-0.5,0, -0.2)

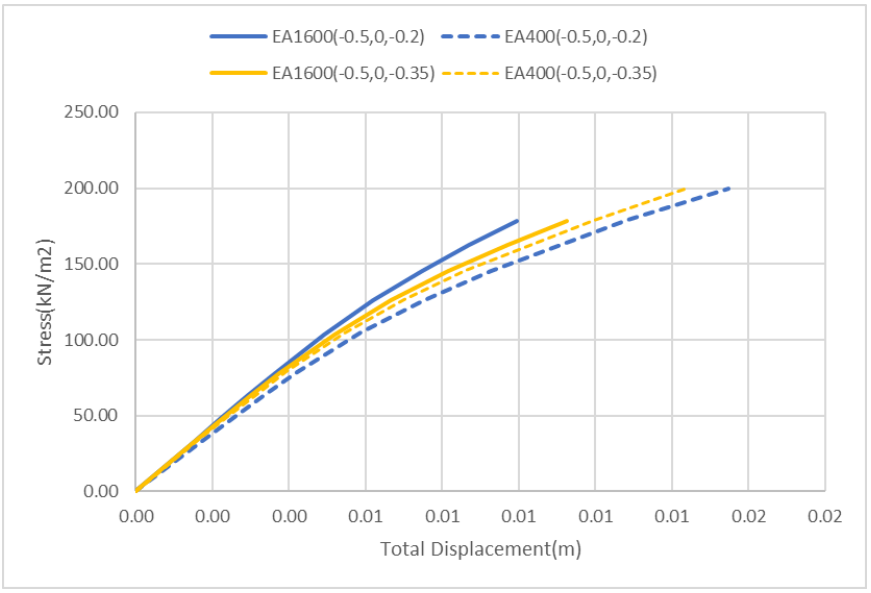

Figure 12: Stress-strain behaviour of reinforced curvilinear geocell with an axial stiffness of 400 and 1600 kN/m at (-0.5,0, -0.2) and (-0.5,0, -0.35)

Case 3.4.3: Axial Stiffness 400 and 1600 kN/m

In this case, the geocell with an axial stiffness of 400 kN/m is compared with that of the geocell with the axial stiffness of 1600 kN/m. In **Figure 12**, the solid line represents the reinforced soil with geocell having the axial stiffness of 1600 kN/m, while the dashed line represents the response of reinforced soil with geocell having the axial stiffness of 400 kN/m. In **Figure 12**, two nodes ((-0.5,0, -0.2) and (-0.5,0, -0.35)) are shown where improvement in the soil is significant that is secant modulus of the reinforced soil with geocell having axial stiffness of 1600 kN/m is higher compared to reinforced soil with geocell having axial stiffness of 400 kN/m. All the nine nodes show improvement in the secant modulus as axial stiffness increase.

Case 3.4.4: Axial Stiffness 400 and 2000 kN/m

In **Figure 13**, the response of the reinforced soil with the axial stiffness of 2000 kN/m is compared with the reinforced soil with geocell having the axial stiffness of 400 kN/m. The two nodes ((-0.5,0, -0.35) and (-0.5,0, -0.2)) out of nine nodes are shown where there is significant improvement due to EA 2000 geocell compared to geocell with axial stiffness of 400 kN/m meaning secant modulus is high in case of geocell with axial stiffness of 2000 kN/m compared to geocell with axial stiffness of a 400 kN/m. The rest of the seven nodes have improvements but are not so significant. On using geocell with an axial stiffness of 2000 kN/m, all the nine nodes show improvement in secant modulus compared to soil with geocell of axial stiffness 400kN/m.

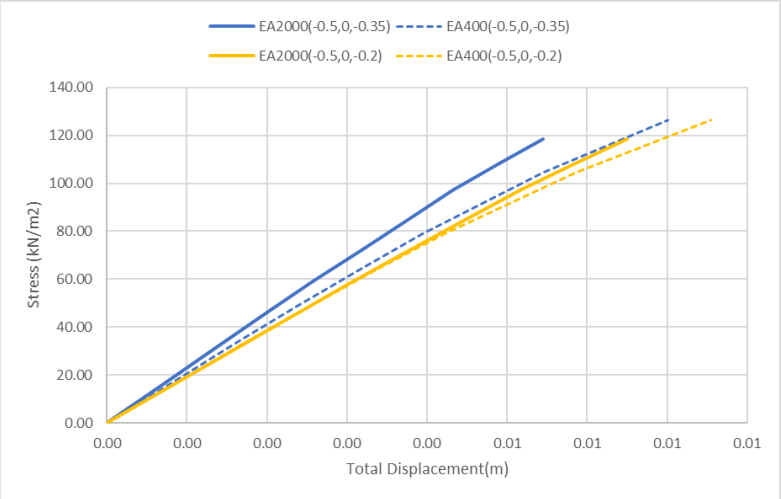

Figure 13: Stress-strain behaviour of reinforced curvilinear geocell with an axial stiffness of 400 and 2000 kN/m at (-0.5,0, -0.35) and (-0.5,0, -0.2)

4 Conclusion

As per mechanism of geocell, the working principle of geocell can be classified into four parts, namely: (1) Shear stress reduction effect, (2) Slab effect, (3) Membrane effect and (4) Interlocking effect. If the geocell is placed too deep, then there is a high chance of failure surface being developed above the geocell and not through the geocell. If the geocell is at a depth above the optimum depth, then there is a chance of a failure surface developing below the geocell. While it is desired that the failure surface goes through the geocell so that maximum utilization of the geocell can occur. In this study, three types of simulations are made, they are: reinforced soil with geocell and unreinforced soil, rectangular geocell with curvilinear geocell, and geocell with a different axial stiffness. The 3D model of the reinforced geocell considering the rectangular shape and curvilinear shape of the geocell is successfully attempted. From the study, it is concluded that as the curvature and the axial stiffness of geocell material increases, the effectiveness of the geocell improves.

5 Reference

1. BaseLok™ Homepage https://baselok.com/geocell/, last accessed 2022/03/05.
2. Bathurst, Richard J., and Rajagopal Karpurapu. "Large-scale triaxial compression testing of geocell-reinforced granular soils." *Geotechnical Testing Journal* (1993): 296-303.
3. Chen, Rong-Her, Yu-Wen Huang, and Feng-Chi Huang. "Confinement effect of geocells on sand samples under triaxial compression." *Geotextiles and Geomembranes* 37 (2013): 35-44.
4. Dash, Sujit Kumar. "Effect of geocell type on load-carrying mechanisms of geocell-reinforced sand foundations." *International Journal of Geomechanics* 12.5 (2012): 537-548.
5. Hegde, A., and T. G. Sitharam. "3-Dimensional numerical modelling of geocell reinforced sand beds." *Geotextiles and Geomembranes* 43.2 (2015): 171-181.
6. Plaxis, 3D. (2015). PLAXIS - PLAXIS 3D Geotechnical Finite Element Software (info). [online]. Available at: http://www.plaxis.nl/plaxis3d/.
7. Shukla, Sanjay, Nagaratnam Sivakugan, and Braja Das. "Fundamental concepts of soil reinforcement—an overview." *International Journal of Geotechnical Engineering* 3.3 (2009): 329-342.